UNIVERSITY OF TWENTE.

Faculty of Electrical Engineering, Mathematics & Computer Science

Measurement Consistency and the Effect of Ground Planes On Common-mode Crosstalk

Georgios Erotas
B.Sc. Thesis
October 2019

Supervisory Committee:
prof. dr. ir. F. Leferink
dr. ir. C. Salm
dr. ir. N. Moonen
J. Lansink Rotgerink, M.Sc.

Telecommunication Engineering Group
Faculty of Electrical Engineering,
Mathematics and Computer Science
University of Twente
P.O. Box 217
7500 AE Enschede
The Netherlands

Measurement Consistency and the Effect of Ground Planes on Common-mode Crosstalk

George Erotas, EEMCS, The University of Twente, the Netherlands

***Abstract*—A comparison between four crosstalk measurement techniques is made to investigate the consistency of the results when the ground plane is highly resistive or missing. The measurement techniques used are: balanced VNA measurements, balanced Spectrum Analyzer measurements, balanced EMI Test Receiver measurements and single-ended measurements converted to mixed-mode. The tests were done on differential pairs of microstrips. It was found that for groundless boards the techniques are still consistent, but the results at high frequencies are greatly dependent on the setup. In case of the carbon fiber ground, the results show matching results for the balanced measurements while the mixed-mode results are consistent in only specific frequency ranges which are dictated by the exact material properties of the CFRP and the directionality of the fibers.**

I. Introduction

The aviation industry is currently involved in the development of electrically propelled aircraft as a potential successor to combustion powered aircraft. As increasing amounts of electrical wiring are added to aircraft, crosstalk is becoming an ever growing concern. Furthermore, most modern aircraft are made partially with carbon fiber. With the use of composites in aircraft being a fairly new practice, a lot of investigation is still required to fully understand its effects. In [1] research was conducted to investigate the effect of carbon fiber ground planes on crosstalk and it was found that a CFRP ground has a mixed result on crosstalk levels, which is frequency dependant and its behavior as a ground plane ranges between a non-conducting ground and a perfectly conducting one. In [2], it was shown that single ended S-parameters can be used to obtain a indication of crosstalk levels under the assumption that there is perfectly conducting ground plane.

As such, an indication exists as to whether the mixed-mode transform will yield valid results for a CFRP ground. In this paper, multiple measurement techniques will be used to assess the effect of a ground plane on the validity of the crosstalk measurements. Specifically, four measurement techniques will be used to measure crosstalk: balanced measurements with a Vector Network Analyzer (VNA) using Baluns, balanced measurement using Baluns with an EMI Test Receiver (transceiver), balanced measurement using Baluns with a Spectrum Analyzer (SA) and lastly the single-ended measurements using the VNA to perform the mixed-mode transform. Three different PCB configurations will be used in order to investigate measurement technique consistency. The aim of this research is to determine in which applications the measurement techniques can be used interchangeably and to examine the effects of the different ground planes.

In Section II the theoretical framework will be presented. Section III describes in detail the measurement setups used along with the design of the PCB boards while Section IV demonstrates the obtained results. Finally, in Section V the results are discussed and Section VI is compromised of the resulting conclusions.

II. Theory and Models

A. Crosstalk Definition

Crosstalk is the undesired electromagnetic coupling which leads to the excitation of a passive line. It is defined as:

$$Crosstalk = 20log_{10}\left(\frac{V_{victim}}{V_{source}}\right) \quad \text{[dB]} \tag{1}$$

with V_{victim} and V_{source} being the voltages of either end of the victim line and the voltage at the excited end of the aggressor line respectively.

B. Common-Mode Pair

In order to simplify the model, the microstrip pair will be modeled as a single conductor. As such, the relation between the per-unit-length (PUL) parameters of single microstrip and the pair has to be examined. The impedance of the pair when it is driven in common-mode is [3]:

$$Z_{comm} = \frac{Z_{even}}{2} \tag{2}$$

with Z_{even} being the impedance of a single line in the presence of the other. It is equal to:

$$Z_{even} = \sqrt{\frac{L_{11} + L_{12}}{C_{11}}} \tag{3}$$

with L_{11} being the self inductance of a single line, L_{12} the mutual inductance of the two parallel lines and C_{11} the self capacitance of a single line. In case there is no coupling between the two lines of the pair, then Eq. 3 would simplify to:

$$Z_{even} = Z_o \tag{4}$$

with Z_o being the characteristic impedance of a single line.

C. The Inductive - Capacitive Model

Crosstalk is calculated with the aforementioned PUL parameters. The following model is an first order approximation based on the model for two single wires as it is presented in [4],[5] and is only valid for common-mode pairs. The internal parameters of each wire are the ones discussed in II-B.

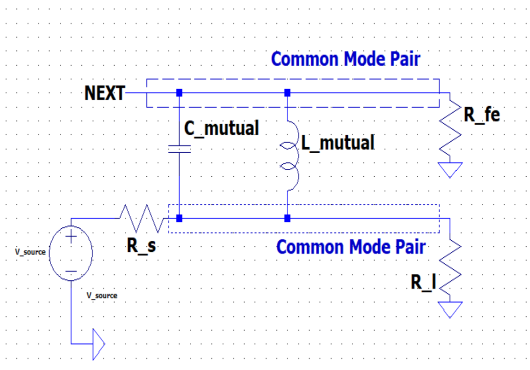

Fig. 1: The simplified model for common-mode NEXT

This model can be found in Figure 1. Each of the elements mentioned in the model have a contribution on the overall crosstalk levels as described below:

- Inductive Coupling, due to the magnetic fields produced by the aggressor line
- Capacitive Coupling, due to the electric fields produced by the aggressor line

All of the following work is done based on the assumptions that the lines are weakly coupled (first order effects are dominant) and electrically short. By solving the multi-conductor transmission line (MTL) equations the following equations are obtained:

$$NEXT = \frac{j\omega(R_{ne}L_m + R_{ne}R_{fe}R_lC_m)}{(R_{ne}+R_{fe})(R_s+R_l)} \tag{5}$$

$$FEXT = \frac{j\omega(R_{ne}R_{fe}R_lC_m - R_{fe}L_m)}{(R_{ne}+R_{fe})(R_s+R_l)} \tag{6}$$

With FEXT being Far End Crosstalk and NEXT Near End Crosstalk. In the above equations, all the parameters are the summations of the PUL parameters and represent the single element equivalents. It has to be noted that the above equations are linear, and not in the form of Eq. 1. From Equations 5 and 6 it can be derived that crosstalk is a linear combination of the discussed mechanisms. Let the ratio r be defined as:

$$r = \frac{R_lR_{fe}}{Z_{cg}Z_{cr}} \tag{7}$$

With R_l and R_{fe} being the termination impedances and Z_{cg} and Z_{cr} being the characteristic impedances of each line in the presence of the other. For r, two distinct cases are of great interest:

$$r < 1 \quad \text{and} \quad r > 1 \tag{8}$$

In the case of r being smaller than 1, then the crosstalk is dominated by the mutual inductance. In the opposite where r is greater than 1, then crosstalk is dominated by the mutual capacitance. It has to be noted that the above model will be used in order to intuitively judge the results, whenever that is possible. In some cases that means that it will be used to describe equivalent phenomena as one of the mechanisms of the model.

D. S-parameters

A VNA will be used, which produces results in the form of S-parameters. This is a deviation from the theory presented in II-C. In contrast, the S-parameter is defined as the ratio of the transmitted and incident power waves between two ports of the system as seen in Eq. 9 [6].

$$S_{ix} = \frac{b_i}{a_x} \tag{9}$$

with b_i and a_x being:

$$b_i = \frac{V_i - Z_i^* I_i}{2\sqrt{|Re(Z_i)|}}, a_x = \frac{V_x + Z_x I_x}{2\sqrt{|Re(Z_x)|}} \tag{10}$$

Equation 9 is only valid if there are no reflections from the loads in the system. This occurs when the impedances are matched (usually $50\,\Omega$). At higher frequencies however, when the terminations do not fully absorb the power signal the S-parameters will start deviating from the definition mentioned in Eq. 9. In that case, the S-parameter has to be calculated through the matrix definition:

$$\boldsymbol{b} = \boldsymbol{Sa} \tag{11}$$

It is also worth noticing that the S-parameter also requires the port local reference conductor in order to be calculated [7].

E. The Mixed-Mode Transform

A useful mathematical transform is the Mixed-Mode S-parameter transform as it allows for the calculation of the balanced equivalents using unbalanced measurements. This is a large benefit, as unbalanced equipment is more easily accessible and the use of frequency limiting elements such as baluns is avoided. This can be done as follows [2]:

$$\boldsymbol{S}_{mm} = \boldsymbol{M}\boldsymbol{S}_s\boldsymbol{M}^{-1} \tag{12}$$

with $\boldsymbol{M}$ being:

$$\boldsymbol{M} = \begin{pmatrix} \boldsymbol{M}_4 & 0 \\ 0 & \boldsymbol{M}_4 \end{pmatrix}, \boldsymbol{M}_4 = \begin{pmatrix} 1 & -1 & 0 & 0 \\ 1 & 1 & 0 & 0 \\ 0 & 0 & 1 & -1 \\ 0 & 0 & 1 & 1 \end{pmatrix}$$

With $\boldsymbol{S}_s$ being the single-ended S-parameter matrix. Using the port definition shown in Fig. 4, the mixed-mode transform matrix mentioned above cannot be used directly. The single S-parameter is first permuted to ensure correct port transformation. This is done by:

$$\boldsymbol{S}_{new} = \boldsymbol{P}\boldsymbol{S}_{old}\boldsymbol{P}^T \tag{13}$$

with $\boldsymbol{P}$ being the following permutation matrix:

$$\boldsymbol{P} = \begin{bmatrix} 1 & 0 & 0 & 0 & 0 & 0 & 0 & 0 \\ 0 & 0 & 1 & 0 & 0 & 0 & 0 & 0 \\ 0 & 1 & 0 & 0 & 0 & 0 & 0 & 0 \\ 0 & 0 & 0 & 1 & 0 & 0 & 0 & 0 \\ 0 & 0 & 0 & 0 & 1 & 0 & 0 & 0 \\ 0 & 0 & 0 & 0 & 0 & 0 & 1 & 0 \\ 0 & 0 & 0 & 0 & 0 & 1 & 0 & 0 \\ 0 & 0 & 0 & 0 & 0 & 0 & 0 & 1 \end{bmatrix}$$

III. Measurements Setup

As mentioned before, the carbon fiber has a behavior that changes with frequency. As such, the two extremities of that behavior are considered in addition to the carbon fiber ground: the case of a non existing ground plane and the case for which there is a copper ground plane.

A. PCB Configurations

The reference board that was used is composed from two pairs of PCB traces with a trace-to-trace distance of $0.15\,\mathrm{mm}$ and pair-to-pair distance of $10\,\mathrm{mm}$. The board is $50\,\mathrm{cm}$ long and the height of the dielectric (FR4) is $0.8\,\mathrm{mm}$. The board was designed to have a common-mode impedance of $25\,\Omega$. Based on this board, three different configurations were made:

- The reference board with a perfect electric conductor (PEC) ground
- A board lacking a ground plane (Free Space Board)
- A board with the ground plane being a generic unidirectional carbon fiber piece (Carbon Fiber Ground)

An image of the boards can be found in Figure 2.

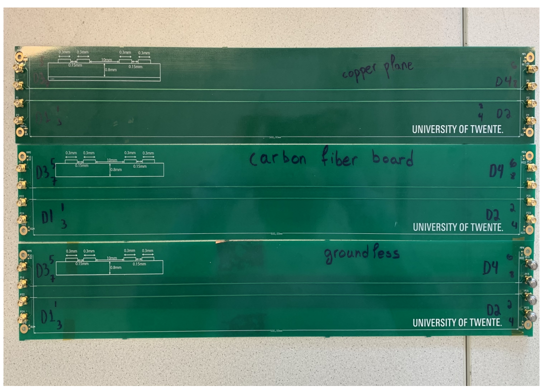

Fig. 2: The board configurations

B. Instruments Used and Settings

For the VNA, a Keysight E5061B Network Analyzer was used. The experiment was performed with the VNA set to 1601 measurement points, $0\,\mathrm{dBm}$ power and 10 times averaging. The transceiver used was the Rohde & Schwarz EMI Test Receiver ESS. The Spectrum Analyzer used was a Siglent SVA1015X and was set to use a resolution bandwidth (RBW) of $120\,\mathrm{kHz}$ and a video bandwidth (VBW) of $100\,\mathrm{kHz}$. The pre-amplifier was turned on to reduce the effect of noise in the results. The tracking generator was set to $0\,\mathrm{dBm}$ power in order to be consistent with the VNA. The selected filter was the EMI filter and the attenuator was automatically set to $30\,\mathrm{dB}$. Lastly, the LCR bridge was the Rohde & Schwarz HM8118 LCR bridge.

C. Balun Selection

The baluns that will be used are the ZFRSC-123-S+ common-mode (CM) power splitter. When using baluns, some limitations have to be considered. In case of the common-mode adapters, they can operate in the range of DC to $12\,\mathrm{GHz}$, so there are no frequency limitations in the range of the measurements. However, in measurements setups that the baluns cannot be removed by calibration then a power loss will be evident. According to the data sheet of the baluns, the average loss is $4.3\,\mathrm{dB}$ per balun. This effect will have to be manually compensated for post measurement.

D. Calibration of the instruments

In order to isolate the behaviour of the boards, the VNA has to be properly calibrated. This was done by performing a SOLT calibration and then using the ”Remove Adapter” setting of the VNA to calibrate post the CM adapters. The resulting forward transmission (S21) result can be found in the Appendix A. When using the EMI transceiver the correction for the balun losses has to be done post measurement. This is done by subtracting the loss that was measured in a THRU with the two baluns connected together. The same procedure was done for the spectrum analyzer, except that the only area calibrated was the frequency range for which the loss is constant. The loss measurements can be found in Figure 14 and 15 of Appendix A.

E. Sketch of the Measurement Setups

The measurements setups for the balanced VNA, transceiver and Spectrum Analyzer are identical with the exception of the instrument used. The instrument is connected to the CM baluns which in turn are connected to the ports of the PCB. Non used ports are terminated with Z_o of $50\,\Omega$ under the assumption that Z_e is also almost equal to $50\,\Omega$. This is illustrated in Fig. 3. In the setup for the single-ended measurements, the VNA is

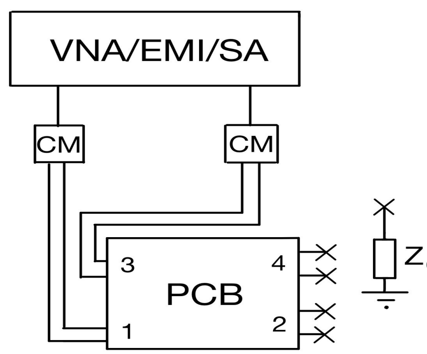

Fig. 3: Setup for balanced measurements

connected to the port pair of interest and all the other ports are terminated with Z_o of $50\,\Omega$. The setup sketch is in Fig. 4.

For both setups, SMA cables and connectors are used.

IV. Results

Common-mode measurements were done with all three boards for NEXT and FEXT. All measurements were conducted with the lines terminated with their characteristic impedance ($50\,\Omega$ for single ended, $25\,\Omega$ for common-mode). The low frequencies (less than $1\,\mathrm{MHz}$) will not be examined for the Spectrum Analyzer since they are an error due to the combination of the large RBW, attenuator settings and the noise floor being at $-70\,\mathrm{dB}$ as seen in Fig. 16.

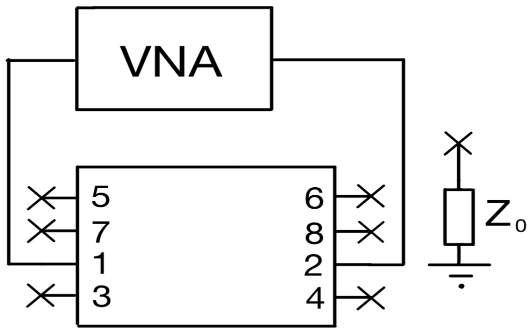

Fig. 4: Setup for single-ended measurements

A. Near End Crosstalk

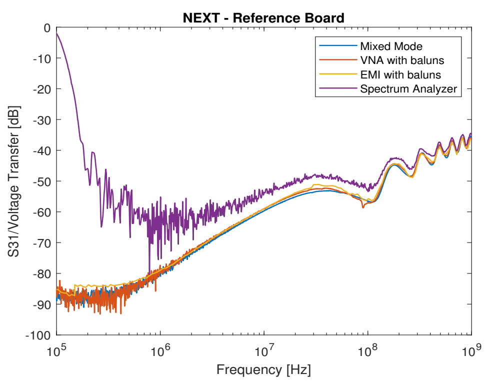

Fig. 5: Reference Board NEXT measurements

Figure 5 clearly indicates the matching measurements from all four techniques. This measurement is to demonstrate that the measurement techniques provide matching results in the ideal case of a perfectly conducting ground plane. This forms the basis that the measurement techniques should provide comparable results. The offset in the spectrum analyzer measurements is $6\,\mathrm{dB}$. In frequencies less than $1\,\mathrm{MHz}$ the VNA measurements show a resistive behaviour but in reality this is the noise floor of the VNA as it was measured in Figure 17.

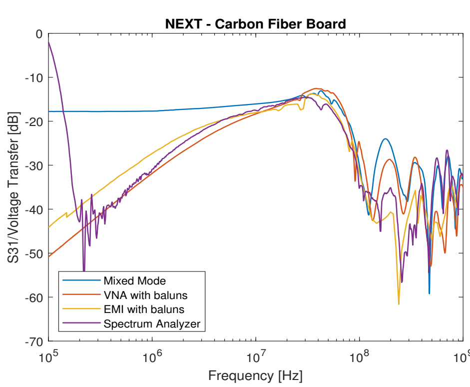

Fig. 6: Carbon Fiber Board NEXT measurements

As it can be seen in Fig. 6, the mixed-mode transform only provides comparable results in the region of $50\,\mathrm{MHz}$ to $1\,\mathrm{GHz}$. In order to investigate this, the ohmic impedance of the carbon fiber slab was measured using a programmable LCR bridge. The data obtained can be found in Appendix A. Judging from that data, the deduction is made that the carbon fiber conducts poorly on lower frequencies. The overall trend however indicates that the conductivity of the carbon fiber improves as frequency increases. Comparing this with the results obtained in Fig. 6, it is possible that from $50\,\mathrm{MHz}$ the carbon fiber behaves as a nicely conducting ground and before that it is not conductive enough for the S-parameters to yield reasonable results. In all cases, the extremities occur on the same frequencies, but there is a large difference in magnitude ($6\,\mathrm{dB}$-$18\,\mathrm{dB}$).

Finally, a transition can be observed at the frequencies of $10\,\mathrm{MHz}$ for the transceiver and CM VNA measurements. This could be possibly due to the presence of the skin effect on the carbon fiber, which can be observed at low frequencies in the cases of carbon fiber [8]. However, it does appear that the transceiver and spectrum analyzer measurements are more susceptible to this effect, while the VNA measurements do not display the same drastic change.

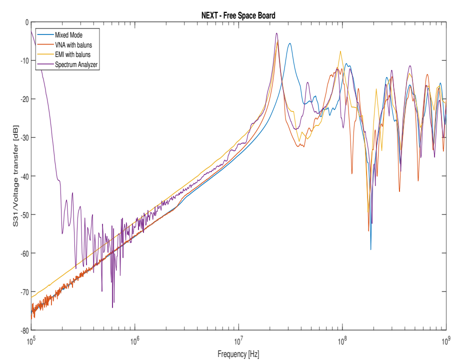

Fig. 7: Free Space Board NEXT measurements

Figure 7 indicates that the case of a groundless board has the highest possible levels of crosstalk. This is to be expected, as there are no ground planes near the conductors which in turn maximizes the effect of cable coupling. Regarding the measurement techniques, the the mixed-mode parameter method to calculate common-mode crosstalk is valid. This is due to the fact that it is not necessary for the grounds of all transmission lines to be the same for the S-parameters to be correctly measured. In fact, the reference of each line is always set by measurement equipment [9] when it is measured. However, in measurements of this type the measurement setup does have an effect on the results. The same measurement was performed again, but this time with the board suspended from the lab table. Figure 8 illustrates the setup.

The results are shown in Figure 9. As it can be seen, the measurement techniques are in agreement again. At this point, an observation about the importance of the specification of the setup can be made. By comparing Fig. 7 and 9 it can be seen that for low frequencies they are identical (up to $23\,\mathrm{MHz}$). At the range of the long line effects however the results are drastically different, due to the different electric permeability of the boxes under the PCB. Based on this observation, it can

Fig. 8: Wooden Boxes used to place the board

be stated that the exact measurement setup in terms of board placement is important to specify the crosstalk levels at higher frequencies. The techniques themselves are consistent.

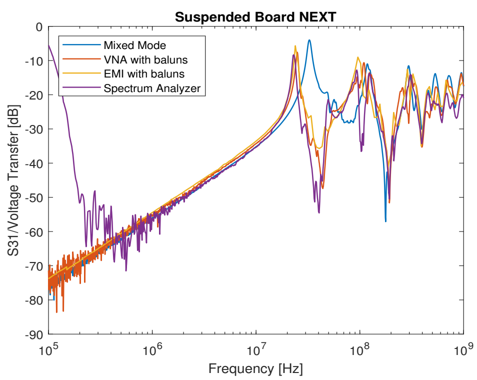

Fig. 9: Suspended Board NEXT measurement

B. Far End Crosstalk

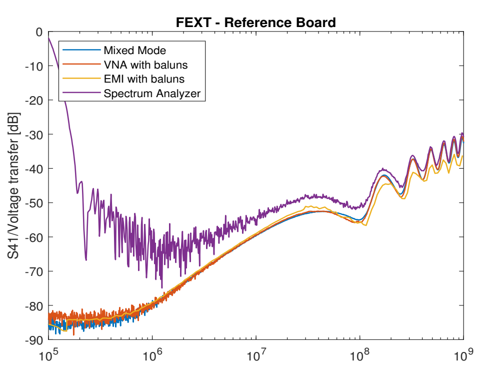

Fig. 10: Reference Board FEXT measurement

As seen also in the near end measurements, when using the reference board the measurement techniques are in agreement as shown in Figure 10.

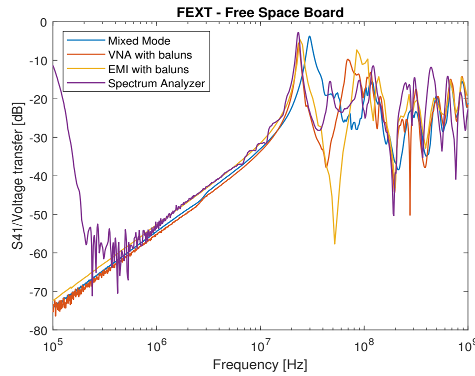

Fig. 11: Free Space Board FEXT measurement

Fig. 11 indicates that n the same fashion as with the NEXT free space measurements, the four techniques provide matching results.

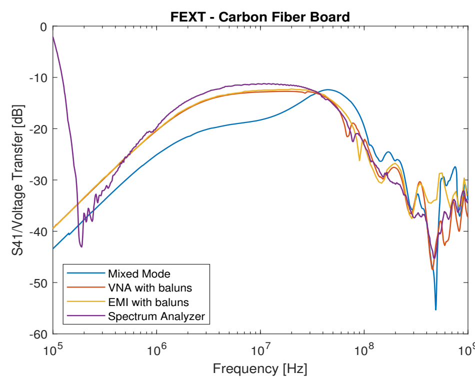

Fig. 12: Carbon Fiber Board FEXT measurement

Unlike for two previous boards, the carbon fiber board demonstrates some large differences between the measurement techniques not previously seen in the near end crosstalk case. In Figure 12, the first striking difference is that the mixed-mode results actually extend to the lower frequencies. This is quite possibly attributed to the inhomogeneous nature of the CFRP. However, they still have a large magnitude difference from the other three techniques. The second point of interest is the plateau at $8\,\mathrm{MHz}$ - $20\,\mathrm{MHz}$. In this region it appears that the crosstalk level is frequency independent, thus demonstrating resistive behavior. The reason behind this is not known, however it could be due to the transition of the carbon fiber from electrically transparent to conductive at those frequencies.

V. Discussion

It has to be noted that some elements that would be useful for drawing further conclusions for the CFRP ground were missing as the ϵ and μ are unknown. This is also one of the points of deviation from the model presented in II-C, which only considers a PEC ground. Also, the impedance of the slab varies depending on the directionality of the fibers. This adds an uncertainty since in the mixed-mode transform measurements the return paths will not have the same properties for each port pair. It might be possible to obtain a model for the impedance of the slab for a given frequency by measuring the impedance between two opposing corners and a diagonal one and using linear interpolation to get a picture of the complete laminate. One of the most troubling results was the fact the carbon fiber slab demonstrates a frequency independent FEXT on a specific range of frequencies. A possible explanation is that the ϵ and μ of the CFRP are greatly dependant on frequency in such a manner that a counter effect is observed between the mutual parameters. A useful future consideration would be to determine the mechanism that makes the NEXT measurement at low frequency completely incorrect, especially since this is not observed in FEXT. The suspicion that this is caused by the directionality of the fibers could be tested by repeating the measurements with a CFRP whose fibers run in the perpendicular direction.

When examining the consistency of the measurement techniques for groundless board measurements, there was a concern that since they is no fixed global reference conductor the S-parameters would yield incorrect results for crosstalk. After investigation it was concluded that the port voltages are referenced to the internal RF ground of the VNA, thus ensuring that there are no floating voltages. Another topic of interest is the single-ended measurement case. Future attention needs to be given to the possible creation of ground loops and their impact on crosstalk measurements.

It could be debated that the Spectrum Analyzer measurements are redundant. By using the tracking generator that is perfectly synced with the analyzer, the setup resembles closely that of an EMI receiver. A more in depth study could be done in the cases that an external source is used, which would most likely result in slightly different results. In addition, a lower RBW setting could be used to get accurate low frequency results at the expense of measurement times.

The last point of interest is the equivalency of the S-parameters and the crosstalk as defined in Eq. 1. Despite the fact that they are used interchangeably in this paper, they are different quantities. In case of matched impedances the S-parameter can be also written as:

$$S_{31} = \frac{V_3 - Z_o^* I_3}{V_1 + Z_o I_1} \tag{14}$$

As it can be seen, the incident voltages and reflected voltages determine the S-parameter. The direct relation between Eq. 1 and 14 is a topic where future research would be required.

VI. Conclusion

It is apparent that for PEC ground planes all measurement techniques are equivalent and can be used interchangeably. When applying those techniques to groundless circuits, they will also be consistent. In high frequencies however, the effect of the setup can clearly be seen. As such, the measurement setup has to be well defined according to set standards and reproduced in order to obtain consistent results and to ensure that the measurements are comparable. Lastly, in cases of CFRP ground planes it is difficult to assess the quality of the results. The balanced measurements are consistent but the mixed-mode transform provides questionable results in lower frequencies but are a good measure of crosstalk in high frequencies. Those frequency ranges in which the mixed-mode measurements are valid are believed to be determined by the electrical properties of the CFRP. As such, an extensive understanding in the nature of the CFRP is also required.

Appendix A
Additional Measurements

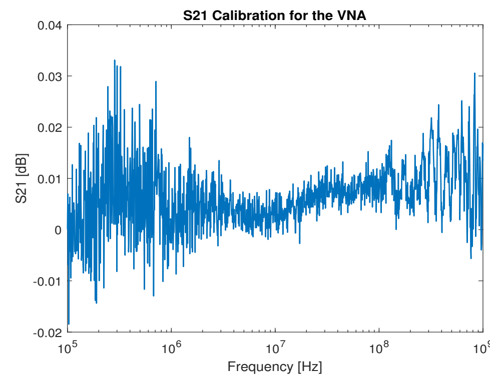

Fig. 13: S21 after calibration

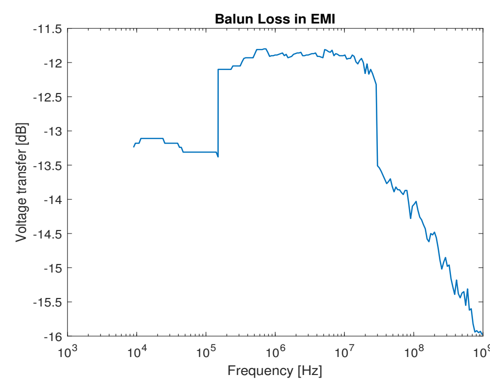

Fig. 14: CM balun loss measurement

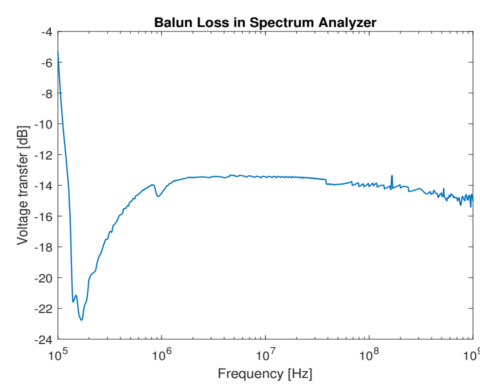

Fig. 15: Balun Effect in the Spectrum Analyzer

Frequency	$Z_{Ground}[\Omega]$
1 kHz	372
10 kHz	325
100 kHz	300

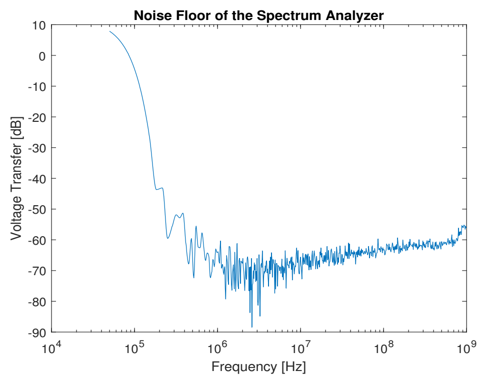

Fig. 16: Noise Floor of the Spectrum Analyzer

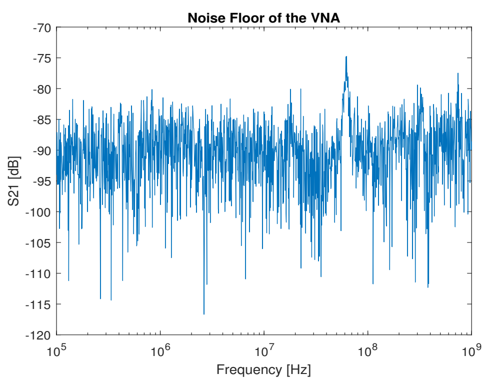

Fig. 17: Noise floor of the VNA

APPENDIX B
MODEL SIMPLIFICATION

The original model for the common-mode pairs can be found in Fig. 18. The mutual inductance and capacitance are excluded from this, as the main point of interest is the transition from two pairs to the equivalent two single conductors. It can be seen that the resistances can be substituted by their equivalents as they are parallel to the ground.

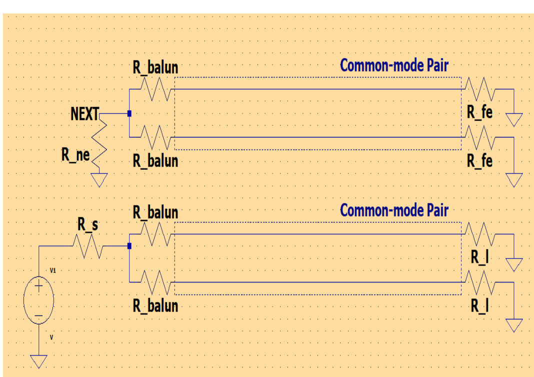

Fig. 18: Model before additional simplifications

REFERENCES

[1] J.H.G.J. Lansink Rotgerink, F. Happ, J.J.P van Es, *Crosstalk between wire pairs above a composite ground plane* , Proc. of the 2016 International Symposium on Electromagnetic Compatibility, 2016.

[2] J.H.G.J Lansink Rotgerink, N. Moonen, F. Leferink, *Mixed-Mode S-Parameter Measurements for Determination of cablie coupling*, 2019 ESA Workshop on Aerospace EMC (Aerospace EMC), 2019.

[3] J. Schutt-Aine, *EELE 461/561 Digital System Design*, Montana State University, 2017.

[4] F. Leferink, *Electromagnetic Compatibility Slides*, Lecture 6, University of Twente, 2019.

[5] C.R. Paul, *Introduction to Electromagnetic Compatibility*, Second Edition, John Wiley & Sons, 2006.

[6] K. Kurokawa, *Power Waves and the Scattering Matrix*, IEEE Transactions on Microwave Theory and Techniques, Vol. 13, No.2, 1965.

[7] E. Bogatin, *Signal and Power Integrity - Simplified*, Chapter 12, Second Edition, Prentice Hall PTR, 2009.

[8] A. Todoroki, *Skin Effect of alternating electric current on laminated CFRP*, Advanced Composite Materials Journal 21 Issue 5-6, Taylor & Francis, 2012.

[9] M. Steinberger, *S Parameter Reference Nodes*, Signal Integrity Software, 2009.